Colloid Polym Sci 274:1006–1011 (1996)
© Steinkopff Verlag 1996

SHORT COMMUNICATION

J. Loos
A. Hückert
J. Petermann

On the crystallization behavior of cold-drawn syndiotactic polypropylene

Received: 27 February 1996
Accepted: 6 May 1996

J. Loos · A. Hückert · Dr. J. Petermann (✉)
Lehrstuhl für Werkstoffkunde
Universität Dortmund
44221 Dortmund, FRG

Abstract The influence of the chain conformation on the crystallization behavior of cold-drawn syndiotactic polypropylene (sPP) has been investigated. The conformational and structural changes depending on drawing conditions and thermal treatments has been observed by x-ray diffraction, infra-red spectroscopy and modulated differential scanning calorimetry. A nucleation and crystal growth model is introduced, which explains the low crystallinity of cold-drawn sPP.

Key words Syndiotactic polypropylene – cold stretching – chain conformation – crystal structure – crystallization behavior

Introduction

Many investigations have been devoted to the relations between crystal structures and their influences on properties of semi-crystalline polymers. The influences can best be demonstrated on polyvinylideneflouride (PVDF) with its helical trans-trans-gauche-gauche $(ttgg)_2$ and all-trans (tttt) conformation in the crystalline state. Only in the all-trans conformation does PVDF have strong piezoelectric and pyroelectric properties and relevant applications [1, 2].

Three different chain conformations in the crystalline state of syndiotactic polypropylene (sPP) have been observed. X-ray structure analysis of sPP by Corradini et al. have revealed a twofold helical $(ttgg)_2$ conformation. Based on this chain conformation, three different crystal structures have been observed, one with isochiral chains packed in a c-centered orthorhombic unit cell (cell I) [3, 4], one with antichiral chains packed along the a-axis of the unit cell (cell II) and the third with antichiral chains packed along a- and b-axes of the unit cell (cell III) [5–8]. Potential energy calculations [9, 10] indicate that nearly equivalent conformational energies of sPP chains are represented by the planar all-trans (tttt) conformation. Samples cold-drawn below the glass transition temperature exhibit a crystal structure based on these zigzag chains [11–13]. Finally, after exposing these specimens to benzene, toluene or p-xylene vapor below 50 °C for several days, the all-trans conformation converts to a $(t_6g_2t_2g_2)$ conformation in the crystalline state of sPP [14].

The influence of the different chain conformations and crystal modifications of sPP on physical properties are still under investigation. It is the purpose of this paper to report some conformational transitions of cold-drawn sPP in connection with its structural characterization.

Experimental

The sPP used in the experiments was kindly supplied by the Fina Oil and Chemical Company. Uniaxially oriented samples were prepared by cold-drawing in a tensile testing machine equipped with a cooling chamber at temperatures of −20 °C and a strain rate of approximately 5%/min. The samples were quenched from the melt into liquid nitrogen before drawing. Immediately after cold-drawing

K 724

and without warming up to room temperature, the samples were fixed between clamps and subsequently annealed at room temperature under constant strain conditions. Heat treatments of some fixed and released samples were carried out in an oven between room temperature and 100 °C.

X-ray measurements were performed at room temperature using a Philips pinhole camera. The thermal testings of the sPP samples were carried out in a TA Instruments differential scanning calorimeter (DSC) 2910 system using both the conventional and the modulated mode at heating rates of 5 °C/min (4 mg sample weight, 50 s modulation period, 0.663 °C modulation amplitude). The theoretical background of modulated DSC is explained in several publications [15, 16]. As described above, all fixed samples were heated from −20 °C to room temperature before the DSC investigations were performed. Only one set of samples was measured immediately after stretching, without fixing and without annealing above −20 °C (in the DSC cell, the samples were free to relax).

The infrared spectra of the stretched samples were performed using a Bio-Rad FTIR165 in transmission mode with a resolution of 2 cm^{-1}. A comparison of the amount of molecules with all-trans chain conformation (wavenumber 867 cm^{-1}) to the amount of crystals formed by molecules with helical chain conformation (wavenumber 962 cm^{-1}) is carried out by comparing the intensities of the respective absorption peaks.

Results

Quenched from the melt, cold-drawing of sPP below its glass transition temperature ($T_G \sim 0$ °C) results in neck formation and propagation. The draw ratio λ between the necks (necked zone) is approximately $\lambda \approx 4$. In the necked zones, a whitened, less optical transparent behavior is visible. Crystals with the planar all-trans conformation, called "all-trans crystals" in this paper, are found in the necked zones of fixed samples after heating them to room temperature. Figure 1 shows an x-ray pinhole fiber diffraction pattern of a low crystallinity specimen with crystals dominantly containing all-trans chains (Fig. 1a) and the corresponding sketch of these patterns with indicated main diffraction reflexes. The diffraction patterns are explained in terms of an orthorhombic cell with cell constants $a = 0.522$ nm, $b = 1.117$ nm and $c = 0.506$ nm [12].

Heat treatments of cold-drawn sPP at different temperatures and preparation conditions were carried out, and result in further information on the crystallization behavior. Annealing at 60 °C (below the supposed melting temperature of the "all-trans crystals") for 1 day provides additional results depending on the sample preparation.

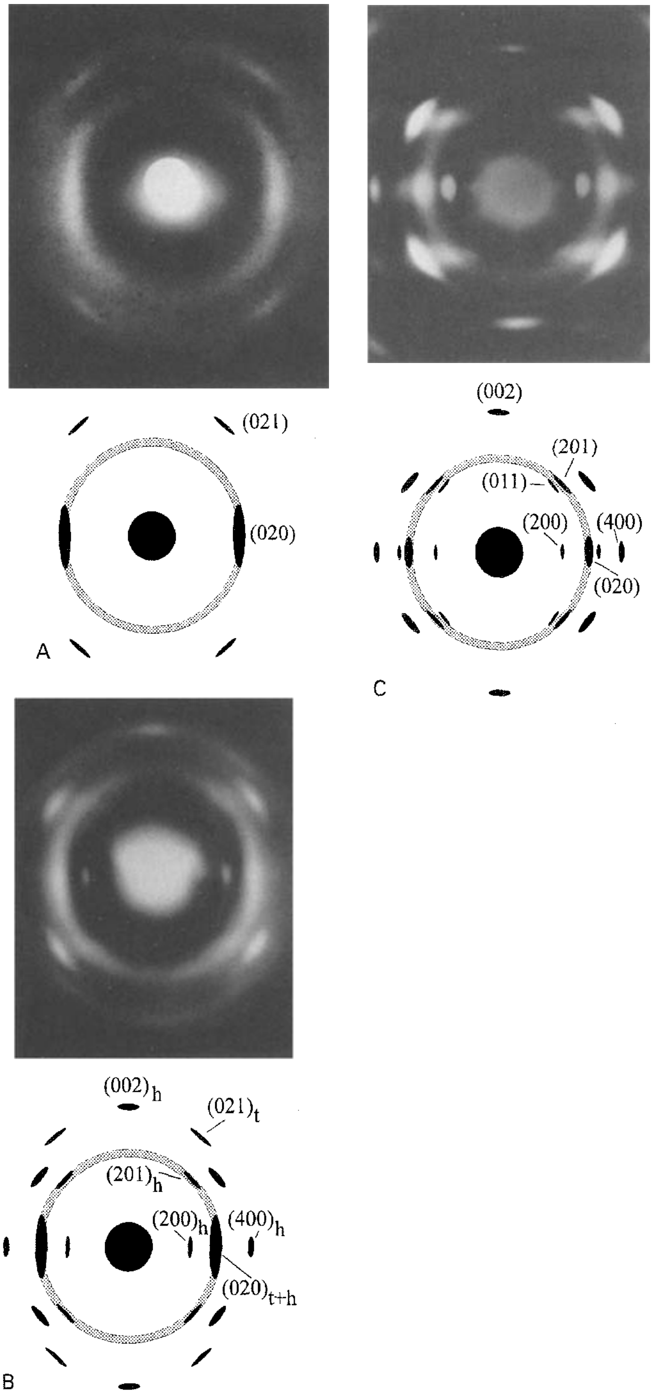

Fig. 1 X-ray pinhole fiber diffraction pattern of cold-drawn sPP: **A** with crystals dominantly built by all-trans chains; **B** relaxed after cold-drawing and annealed at 60 °C for 1 day; **C** annealed at 100 °C; the most intense reflections are indexed in the corresponding sketches (t = all-trans; h = helical)

Samples fixed between clamps during that heat treatment reveal no increase in the planar "all-trans crystallinity" and the x-ray diffraction pattern is comparable with Fig. 1a.

The same heat treatment with relaxed samples exhibit shrinkage and leads to a change in the x-ray diffraction pattern (Fig. 1b, with corresponding sketch). Reflexes of both oriented "all-trans crystals" and crystals containing molecules with helical conformation, called "helical crystals" in this paper, are recognizable. The (020) meridian reflections and the (021) reflection of the orthorhombic "all-trans form" and, for example, the (200) and (002) reflections of the orthorhombic "helical crystal form" of the cell I and II type are visible, with cell constants $a = 1.45$ nm, $b = 0.56$ nm and $c = 0.74$ nm. Annealing at 100 °C, the x-ray pinhole diffraction patterns of cold-drawn sPP indicate a high degree of oriented "helical crystals" (Fig. 1c, with corresponding sketch). Reflections of the orthorhombic all-trans form are completely absent. Compared to Fig. 1b, the additional (011) reflections of the cell III form is visible and the diffraction patterns are explained in terms of an orthorhombic cell with cell constants $a = 1.45$ nm, $b = 1.12$ nm and $c = 0.74$ nm.

Further information on the crystallization behavior of cold-drawn sPP are carried out by conventional DSC measurements. For comparison, the crystallization and melting behavior of a melt quenched, not deformed sPP sample was recorded and is shown in Fig. 2a. Starting at −20 °C, the sample exhibits at 0 °C its glass transition and at 35 °C a crystallization maximum, followed by the melting of "helical crystals."

While all other cold-drawn samples were exposed before the DSC measurements to room temperature under constant strain conditions, one sample was transferred to the DSC without being exposed to a temperature higher than the deformation temperature (Fig. 2b) and having the same thermal history as the drawn strained sample. After a glass transition at 0 °C, a crystallization exotherm is seen as in the non drawn sample, but at 30 °C. Its melting endotherm peak is at somewhat higher temperature than that of the non drawn sample and the enthalpy of melting (area under the melting peak) also seems to be larger.

The crystallization and melting behavior of a cold-drawn sPP sample, exposed before the DSC measurements to room temperature under constant strain conditions, is shown in Fig. 2c. The crystallization occurred during the exposure to room temperature outside the DSC. After the glass transition at 0 °C, an exothermic peak in a temperature range between 70° and 100 °C is visible, followed by the double melting peak of cell II and cell III "helical crystals".

Annealing the deformed samples at 60 °C under constant strain conditions for 1 day gives no change in the DSC traces compared to the samples annealed at room temperature (Fig. 2c). The same heat treatment but with free ends leads in the DSC traces to an additional endothermic peak at 75 °C (Fig. 2d). Annealing the samples with free and fixed ends at 100 °C results in DSC traces as shown in Fig. 2e.

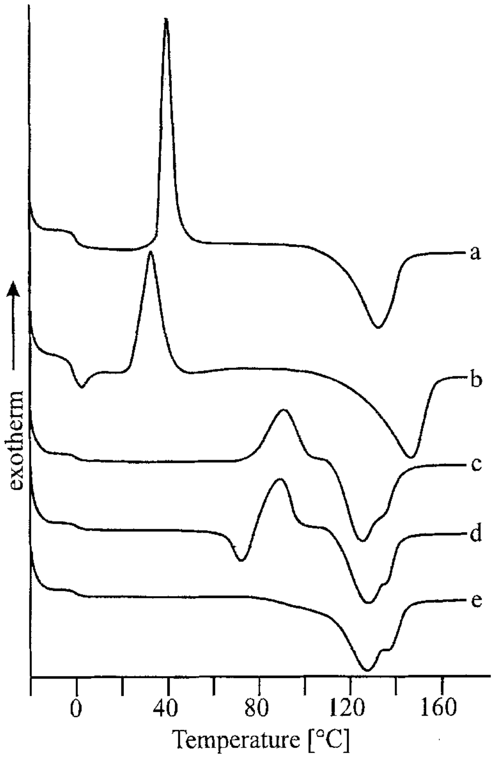

Fig. 2 DSC traces of sPP samples: a) glassy, non-oriented; b) cold-drawn and immediately measured without interruption of the cooling below T_G; c) cold-drawn and annealed under constant strain at room temperature; d) cold-drawn and fixed during annealing at RT, then released and annealed at 60 °C for 1 day; e) cold-drawn and fixed during annealing at RT, then annealed at 100 °C

Simultaneously, the thermal behavior of cold-drawn sPP was studied by modulated DSC investigations. Using the modulated DSC, measurements yield additional information about the thermal behavior of the samples. An advantage of modulated DSC is its ability to disentangle overlapping processes. As an example, in polyethyleneterephthalate it is known that a process of melting and subsequent recrystallization occurs simultaneously at temperatures where small, imperfect crystals start to melt at rather high undercooling and immediately crystallize again into larger, more perfect crystals [17]. This process is not detectable by conventional DSC but may be resolved by modulated DSC. The adjustments of the parameters (modulation periods, temperature amplitude and heating rates) in the modulated DSC are very critical and have to be fitted to the thermal process under investigation. As the interpretations of the data are still under debate, only qualitative results are presented here, and their interpretations have to be seen in close connection to

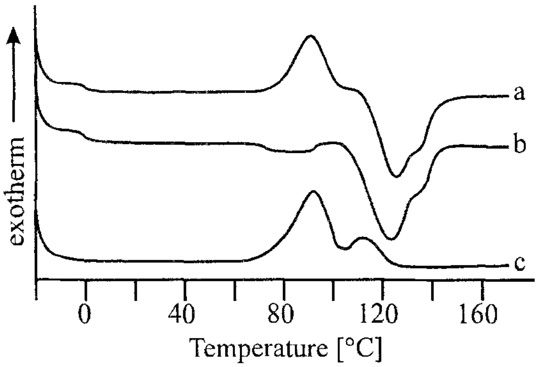

Fig. 3 Modulated DSC traces of cold-drawn sPP: a) total heat flow; b) reversing heat flow; c) non-reversing heat flow

the x-ray diffraction patterns. The transformation of the all-trans crystals in the cold drawn sample into crystal modifications with helical chain conformations occurs in a temperature range between 70° and 100 °C (Figs. 1b, c). The conventional DSC exhibits in this temperature range an exothermic heat flux (Fig. 2c).

Figure 3 shows the three simultaneously measured modulated DSC traces of the total (Fig. 3a), the reversing (Fig. 3b) and the non-reversing heat flow (Fig. 3c) of cold-drawn sPP (Fig. 3a is equivalent to Fig. 2c). As the frequency of the modulation is 0.8 min^{-1}, about seven modulations in the temperature range between 70° and 100 °C occur, which may be enough for a realistic Fourier transform. The reversing heat flow indicates changes of the heat capacity, like glass transition or melting, and the measured reversing heat flow shows at 0 °C the glass transition and an endothermic behavior between 70° and 100 °C. In comparison with the enthalpy of the exothermic behavior of the total heat flow, the enthalpy in the reversing heat flow between 70° and 100 °C is low. The third trace shows the non-reversing heat flow and indicates kinetically determined transitions, like crystallization. It is calculated from the difference of the total heat flow minus the reversing heat flow and shows two exothermic crystallization events, between 70° and 110 °C. The first is the crystallization of the cell II and III modification, the second the recrystallization of cell III "helical crystals." As mentioned above, no quantitative results should be drawn from this measurements.

In Table 1, the ratios of the intensities of the absorption bands at 867 cm^{-1} (resulting from vibrations of the all-trans conformation) and at 962 cm^{-1} (resulting from the helical conformation) are listed for cold-drawn samples annealed at room temperature and at 60 °C for 1 day under constant strain conditions and at 60 °C under relaxed conditions. An increase of the intensity of the 962 cm^{-1} band with annealing temperature, especially under relaxed conditions, was observed.

Table 1 Calculated relation of the amount of macromolecules with all-trans conformation with the amount of crystals built by molecules with helical conformation for different preparation conditions

cold-drawn, fixed ends	fixed ends annealed at 60 °C	released, annealed at 60 °C
2.15 ± 0.06	1.99 ± 0.09	1.23 ± 0.23

Discussion

As already reported by Natta et al., sPP can crystallize in modifications containing the all-trans conformation of the sPP chain [4] or the helical conformation [3]. Potentional energy calculations have indicated that the potentional energies of both chain conformations are nearly identical [9, 10], and recent NMR measurements documented that amorphous sPP contains a high amount of all-trans segments [18]. But the crystallization of sPP from the melt or the non-oriented glassy state results in "helical crystal" modifications of cell I, II or III. Presently, the only way to obtain the orthorhombic crystal modification with the all-trans conformation is after stretching the amorphous material below its glass transition temperature [19, 20]. But as concluded from our DSC results (Fig. 2b), the crystallization occurs after cold stretching by heating above the glass transition temperature under constant strain. The crystallinity of those oriented samples is surprisingly low compared to samples, which were crystallized at the same temperature (for example, room temperature) from the non-oriented amorphous state. Generally, in other semi-crystalline polymers the opposite effect is observed: highly oriented polymeric material exhibits higher or as high crystallinity as material crystallized from the non-oriented state under otherwise the same conditions.

The low crystallinity of our strained samples can be estimated from the melting endotherm seen in the reversing part of the modulated DSC (Fig. 3b) and the x-ray diffraction patterns (Fig. 1a). No exact values of the crystallinities should be calculated from our results; because pinhole x-ray photographs are not suitable, the excess enthalpies of the conventional DSC measurements consist of overlapping thermal transformations and the data of the modulated DSC are too uncertain to draw quantitative conclusions. It still remains to be explained why the crystallinity is so low. The material used in our investigation is a pre-commercial product with a syndiotactic pentads content (rrrr) in the range of 85–90%, resulting in an average syndiotactic sequence length of approximately 50 monomers [21]. This corresponds to an average perfect syndiotactic chain segment length below 11nm. From this estimation it may be speculated that only a small fraction of the sPP chains have perfect syndiotactic sequence length larger than the critical nucleus size and, hence, are able to form configurational defect-free crystals.

An extended syndiotactic chain containing an "isotactic monomer" changes in its all-trans conformation its spatial direction, while in the helical conformation only the chirality of the chain to opposite handedness is changed, but the coaxial direction is maintained [22, 24]. An "isotactic monomer" within a syndiotactic extended polymer chain with all-trans conformation is therefore incompatible with a crystal, while it acts only as a linear defect in its helical conformation and may cause the occurrence of the less ordered crystal modifications of cell I or cell II. It is therefore to be expected that sPP with higher configurational perfection will lead to higher crystallinity for the all-trans crystal modification and higher cell III content for the helical crystals.

The overall crystallization behavior of cold stretched sPP results in the orthorhombic crystal modification with the helical chain conformation when the sample is free to relax, and in the orthorhombic crystal modification with all-trans chain conformation, when the sample crystallizes under constant strain (Figs. 2b and 2c). This crystal modification melts between 70° and 90 °C but recrystallizes spontaneously at the same temperature into the cell II and cell III modification (Fig. 3).

The low all-trans crystallinity of the samples results in a rubber-like mechanical behavior, were the all-trans crystals act as crosslinks of the matrix (Fig. 4a) [24, 25] and the amorphous matrix is spatially hindered to crystallize, as the space between the crystals is too small to form "helical crystals". Annealing those samples free to relax below the melting range of the "all-trans crystals" and cooling them to room temperature leads to a two crystal phase structure of "all-trans" and "helical crystals" of cell I and II (Figs. 1b, 4b and Table 1). The higher the annealing temperature, the more thermally stable the crystals. But generally it was observed that their melting occurred about 10 °C above their crystallization temperature (Fig. 2d is an example for 60 °C annealing temperature). Samples with fixed ends do not show the effect till the temperature of the melting range of the "all-trans crystals." This may be explained by the restricted mobility of the tie chains between the "all-trans crystals" under the constant strain condition. Annealing above the melting range of the "all-trans crystals" results in the formation of highly oriented "helical crystals" with the cell II and III modification (Figs. 1c, 2e and 4c). This process occurs by a simultaneous melting and recrystallization of the "all-trans" and small "helical cell I and II crystalls." The cell III formation (compared to the isothermal crystallization from the relaxed melt) is favored by the selection of "perfect syndiotactic" sequences in areas of the molten "all-trans crystals," which may form the nuclei of the cell III crystals.

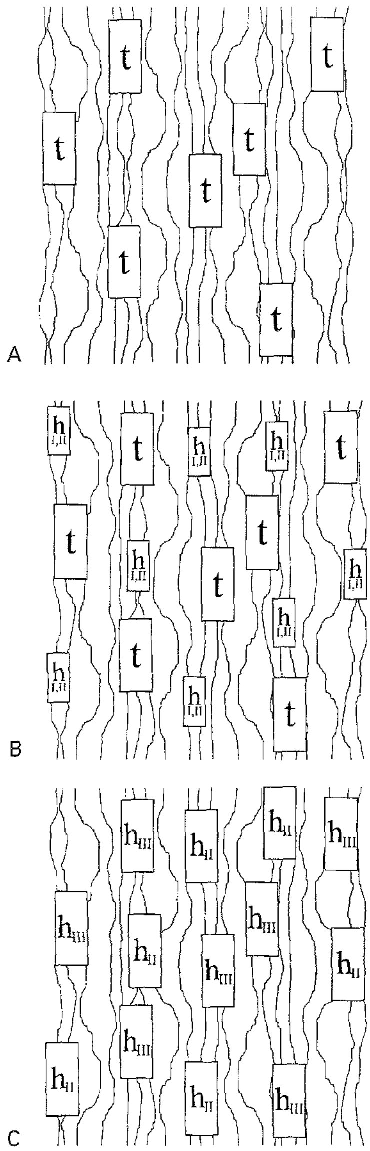

Fig. 4 A model of the crystalline morphology of cold-drawn sPP annealed under fixed ends above T_G and below 80 °C (*t* corresponds to "all-trans crystals," *h* to "helical crystals" of cell I, II or III) : **A** exposed to room temperature under constant strain conditions; **B** annealed free to relax between room temperature and 60 °C; **C** annealed above 100 °C

Further investigations are necessary using sPP with higher syndiotactic pentad contents in order to distinguish between crystal formations caused by thermodynamic reasons and by configurational defect restrictions.

Conclusion

A model of the crystallization of cold stretched (below T_G) and subsequently annealed sPP samples is presented. The crystallization occurs within three steps:

1) At low temperatures "all-trans crystals" are formed and are thermally stable to about 70 °C.

2) Additional crystallization of "helical cell I and II crystals" occurs when the samples are annealed free to relax in a temperature range between room temperature and 60 °C. No such crystallization occurs of fixed samples.

3) Annealing the samples above 100 °C results in the disappearance of both the all-trans and the helical cell I crystal modifications, and in the formation of "helical cell II and III crystals."

The crystallization behavior can be understood, when taking the perfection of the tacticity of the chains into account.

Acknowledgment This study was supported by the Deutsche Forschungs Gemeinschaft (DFG). We also wish to thank the Fina Oil and Chemical Company for supplying the sPP material. The authors also thank the Institute of Material Science, University of Bochum, Germany, for help and support.

References

1. Lovinger AJ (1983) Science 220:1115
2. Hasegawo R, Takahashi Y, Chatani Y, Tadokoro H (1972) Polymer Journal 3:600
3. Corradini P, Natta G, Ganis P, Temussi PA (1967) J Polym Sci, Part C 16:2477
4. Natta G, Pasquon I, Corradini P, Peraldo M, Pegoraro M, Zambelli A (1960) Rend Acc Naz Lincei 28:539
5. Lotz B, Lovinger AJ, Cais RE (1988) Macromolecules 21:2375
6. Lovinger AJ, Lotz B, Davis DD (1990) Polymer 31:2253
7. Lovinger AJ, Davis DD, Lotz B (1991) Macromolecules 24:552
8. De Rosa C, Corradini P (1993) Macromolecules 26:5711
9. Natta G, Corradini P, Ganis P (1960) Macromolecules 39:238
10. Natta G, Corradini P, Ganis P (1962) J Polym Sci 58:1191
11. Natta G, Peraldo M, Allegra G (1964) Makromol Chem 75:215
12. Chatani Y, Maruyama H, Noguchi K, Asanuma T, Shiomura T (1990) J Polym Sci, Part C: Polym Lett 28:393
13. Tadokoro H, Kobayashi M, Kobayashi S, Yasufuku K, Mori K (1966) Rep Prog Polym Phys Jpn 9:181
14. Chatani Y, Maruyama H, Asanuma T, Shiomura T (1991) J Polym Sci, Part B: Polym Phys 29:1649
15. Reading M (1993) TRIP 8:248
16. Boller A, Jin Y, Wunderlich B (1994) J Thermal Anal 42:307
17. Wunderlich B (1990) In: Thermal Analysis. Academic Press, Boston
18. Sozanni P, Simonutti R, Galimberti M (1993) Macromolecules 26:5782
19. Natta G, Peraldo M, Allegra G (1965) Makromol Chem 75:215
20. Tadokoro H, Kobayashi M, Yasufuku K, Mori H (1966) Rep Prog Polym Phys Jpn 9:181
21. Paukkeri R, Väänänen T, Lehtinen A (1993) Polymer 34:2488
22. Auriemma F, De Rosa C, Corradini P (1993) Macromolecules 26:5719
23. Ammendola P, Shijing X, Grassi A, Zambelli A (1988) Gazz Chim Ital 118:769
24. Bonart R (1979) Polymer 20:1389
25. Loos J, Ebener H, Petermann J, in preparation